Microscopy Image Enhancement for Cost-Effective Cervical Cancer Screening

Joakim Lindblad[1(✉)], Ewert Bengtsson[2], and Nataša Sladoje[2,3]

[1] Faculty of Technical Sciences, University of Novi Sad, Novi Sad, Serbia
joakim@cb.uu.se
[2] Centre for Image Analysis, Department of Information Technology, Uppsala University, Uppsala, Sweden
ewert@cb.uu.se
[3] Mathematical Institute, Serbian Academy of Sciences and Arts, Belgrade, Serbia
natasa.sladoje@it.uu.se

Abstract. We propose a simple and fast method for microscopy image enhancement and quantitatively evaluate its performance on a database containing cell images obtained from microscope setups of several levels of quality. The method utilizes an efficiently and accurately estimated relative modulation transfer function to generate images of higher quality, starting from those of lower quality, by filtering in the Fourier domain. We evaluate the method visually and based on correlation coefficient and normalized mutual information. We conclude that enhanced images exhibit high similarity, both visually and in terms of information content, with acquired high quality images. This is an important result for the development of a cost-effective screening system for cervical cancer.

1 Introduction

In microscopy, very high quality optical systems are considerably more expensive than those of a standard quality; significant reduction in overall system cost can be achieved if cheaper optics can be utilized without sacrificing too much of performance. Similarly, when facing large scale imaging tasks, there is also a trade of regarding the number of pixels to utilize and the reached processing speed. Decreasing the pixel size by a factor two, in order to increase the amount of image detail, leads to an increase in the number of pixels to process by a factor of four. This often translates to a corresponding increase in operational costs of the system.

We are working on a project to design a cost-effective screening system for cervical cancer, based on the detection of subtle malignancy associated changes (MAC) in the chromatin structure of cell nuclei, imaged using bright-field microscopy [7]. An example of our image material is shown in Fig. 1. For a successful differentiation of chromatin distribution seen as nuclear texture properties of the observed samples, it is essential to work with images of a quality sufficient to resolve the details needed for the analysis. On the other hand, to enable efficient processing of the acquired data, where the number of images to

R.R. Paulsen and K.S. Pedersen (Eds.): SCIA 2015, LNCS 9127, pp. 440–451, 2015.
DOI: 10.1007/978-3-319-19665-7_37

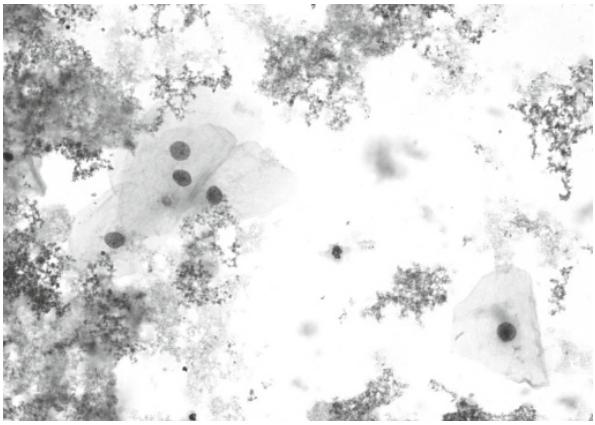

Fig. 1. Part of a PAP-smear, imaged with extended depth of focus

analyse is typically very high, the size of images, in terms of number of pixels, must be reasonable.

To keep costs at a reasonable level, a good balance between the quality of data and the cost of its processing is a necessity. In the cervical cancer screening study we work on, we have observed a satisfactory performance when utilizing images acquired using a high quality setup with a top of the line lens at 40×. The system would become significantly more cost-effective if we could, e.g., instead use a more standard lens at 20×. The secondary magnification, which determines final pixel size, also has to be optimized. The quality of the acquired images is affected by several different parameters of the imaging system and the overall performance optimization is a rather challenging task. An example showing one cell nucleus, extracted from images acquired by seven different microscopy configurations is shown in Fig 2.

To maximize the performance of the analysis, two approaches can be followed: (i) To develop feature extraction methods with increased precision and robustness, and make them suited for efficient analysis of lower quality images; (ii) To enhance image quality (to reduce noise and effects of limited resolution) by utilizing appropriate image processing methods, so that application of classical feature extraction methods provides satisfactory results.

We proposed in [6] a method for generating images at lower optical resolution, starting from higher quality ones, based on an efficient estimation of the relative modulation transfer function (RMTF). This facilitates evaluation of feature estimation methods in terms of robustness w.r.t. change of image quality and resolution. The method has shown to work very well; features estimated from synthesized images closely resemble those of real images acquired at the (low) goal resolution.

In this paper we follow the second track, that is, we aim to enhance the quality of acquired images and by that enable better subsequent analysis by classical image analysis methods. We use the same idea as in [6], but now we utilize the

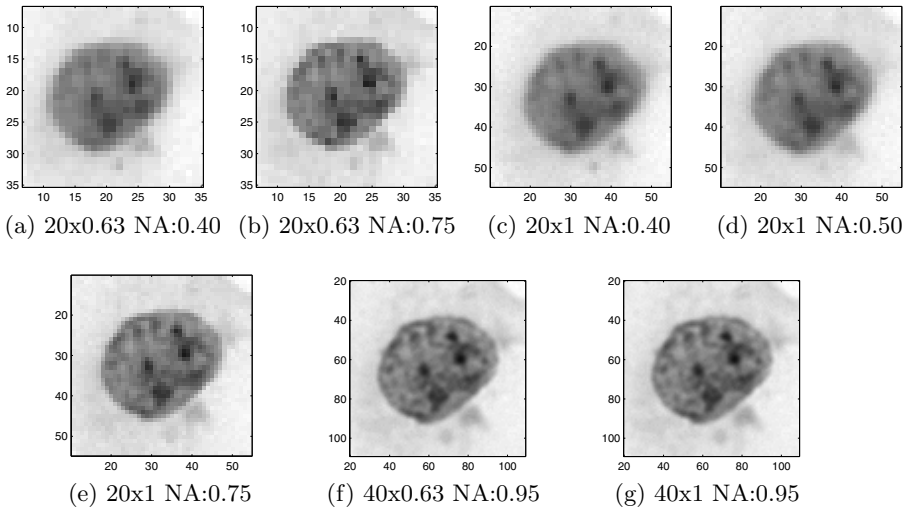

(a) 20x0.63 NA:0.40 (b) 20x0.63 NA:0.75 (c) 20x1 NA:0.40 (d) 20x1 NA:0.50

(e) 20x1 NA:0.75 (f) 40x0.63 NA:0.95 (g) 40x1 NA:0.95

Fig. 2. Examples of one extracted cell nucleus from images acquired by the seven used microscopy configurations. For display purposes the images are magnified to the same size; the actual image matrices vary significantly in size.

estimated RMTFs to enhance low quality images, rather than degrade high quality ones. This is of course a much more challenging task; it is well known that the image deconvolution problem is, in the presence of noise, numerically unstable, often leading to severe problems with exploding noise levels. Image deconvolution and denoising are therefore typically done by iterative procedures and utilizing some a priori knowledge of the system. Approaches based on sparse regularized energy minimization are numerous and very popular [5,9,10]. However, they are also relatively complex and computationally demanding. The approach that we propose in this paper is based on direct multiplication in the Fourier domain. It is fast and simple, and offers an appealing balance between performance and cost. Explicit usage of the transfer functions of individual optical systems is avoided. Instead, the method relies on the estimated relative transfer functions between microscope setups, which limits the noise magnification and provides excellent results for our task. This is confirmed by the conducted quantitative evaluation.

2 Background and Previous Work

The point spread function (PSF) is the spatial response of an imaging system to a point light source; knowledge of the PSF reveals how sharp details can be reproduced by the imaging system. The (complex valued) system optical transfer function (OTF), is the Fourier transform of the system PSF. The modulation transfer function (MTF) is the modulus of the OTF, and is the most fundamental descriptor of the performance of an optical system. In this work we observe the

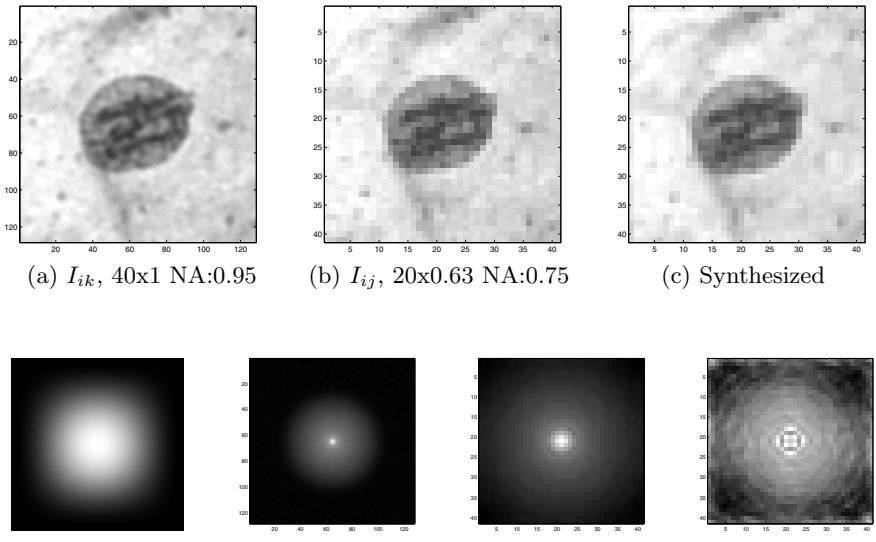

(a) I_{ik}, 40x1 NA:0.95 (b) I_{ij}, 20x0.63 NA:0.75 (c) Synthesized

(d) Hann window (e) AvgMTF$_j$ (f) AvgMTF$_k$ (g) RMTF

Fig. 3. (a) Initial (sensed) high resolution image I_{ik} acquired using a high quality 40× lens. (b) Reference image at desired goal quality I_{ij} acquired with a cheaper 20× lens and a lower sampling rate. (c) Synthesized reduced quality image $\tilde{I}_{ij}$ according to (5). (d) Used spatial weighting function, a 2D Hann window. (e,f) Average MTF of setups j and k. (h) Estimated RMTF H_{kj} according to (4).

ratio of the MTFs between different imaging systems, which we refer to as the relative modulation transfer function (RMTF).

An intuitive approach to take, in order to generate images simulating different image acquisition conditions, is to first estimate the PSF of each optical setup and then to utilize them to deconvolve an initial image by the source PSF and then convolve with the destination PSF. Accurate estimation of the PSF, however, is for a number of reasons, a very challenging tasks. We have found method relying on edge model assumptions and/or regularized energy minimization both difficult to use in practice and often providing results of not high enough quality [4,12]. We have proposed a parameter free method to directly estimate the difference in performance between different setups, instead of trying to extract an absolute characteristics of each optical setup separately, [6]. By this, we avoid a number of difficulties and approximations leading to imprecision. In the following we briefly recall the details of the RMTF estimation.

2.1 Relative Modulation Transfer Function Estimation and Generation of Reduced Quality Images

Following [6], we denote by I_{ij} an image of a specimen i, captured with an optical setup j. The acquired image I_{ij} is a result of a convolution of the intensity

function of the imaged scene/specimen S_i with the PSF P_j of the used imaging device, $I_{ij} = S_i * P_j$. The same relation expressed in the frequency domain is given by a pointwise multiplication, $F_{ij} = \mathcal{S}_i \cdot O_j$, where F_{ij} is the Fourier transform of the image I_{ij}, $F_{ij} = \mathcal{F}(I_{ij})$, $\mathcal{S}_i$ is the spectral representation (Fourier transform) of the scene S_i, and O_j is the OTF of the device (setup) j. Given F_{ik}, originating from an image of the same scene S_i, but acquired using a different optical configuration k, the spectral representation F_{ij} can be expressed as

$$F_{ij} = \mathcal{S}_i O_j = \mathcal{S}_i O_k \frac{O_j}{O_k} = F_{ik} \frac{O_j}{O_k} \,. \tag{1}$$

The *relative OTF*, describing what differentiates two imaging systems, can be estimated from the collection of values F_{ij}, without explicit knowledge of the scenes S_i. Assuming that we have acquired images of one same scene S_i by optical setups j and k, we can compute

$$\frac{O_j}{O_k} = \frac{F_{ij}\mathcal{S}_i}{F_{ik}\mathcal{S}_i} = \frac{F_{ij}}{F_{ik}} \,. \tag{2}$$

To reduce edge effects and sensitivity to displacements of the scenes, we first multiply each image in the spatial domain with a 2D Hann window. We further reduce translation sensitivity by ignoring the phase component of the system. Thus, observing the magnitude of the spectra, we obtain the formula for the relative modulation transfer function H_{kj}:

$$H_{kj} = \frac{|O_j|}{|O_k|} = \frac{|F_{ij}|}{|F_{ik}|} \,. \tag{3}$$

To ensure numerical stability and reduce noise sensitivity, we use the fact that the MTFs of the different setups are spatially invariant and do not depend on the imaged specimen, which allows averaging over several images. By summing magnitude spectra, we also ensure that values do not cancel each other.

A simple, robust and effective formula for estimating the relative transfer function is given in [6] as

$$H_{kj} = \frac{\sum_{i=1}^{m} |F_{ij}|}{\sum_{i=1}^{m} |F_{ik}|} \,, \tag{4}$$

where m is the number of different specimen imaged by each of the different setups.

To generate synthetic images at optics quality j, starting from images acquired by a setup k, it is sufficient to filter the Fourier transform of the initial image by the appropriate relative transfer function, and compute the inverse Fourier transform ($\mathcal{F}^{-1}$) of the result:

$$\tilde{I}_{ij} = \mathcal{F}^{-1}(\mathcal{F}(I_{ik}) \cdot H_{kj}) \,. \tag{5}$$

An example of generating an image of a lower quality starting from a high quality one by utilizing the estimated RMTF and Eq. (5) is illustrated in Fig. 3.

3 Algorithm for Enhancement of Microscopy Images Acquired with Different Setups

The objective of this publication is different from that of [6]; our aim now is image enhancement, i.e., we wish to synthesize a higher quality image starting from a lower quality one. This is an ill-posed problem that we address by utilizing efficiently estimated RMTF, as described in the previous section. The enhanced image is determined as

$$\tilde{I}_{ij} = \mathcal{F}^{-1}(\mathcal{F}(I_{ik}) \cdot H_{kj} \cdot BW_{jk}) \,. \tag{6}$$

where $\mathcal{F}^{-1}$ is the inverse Fourier transform and BW_{jk} is a 7-th order Butterworth filter with a cutoff frequency at 0.95 times the Nyquist frequency of the smaller of the two images j and k. The included Butterworth filter reduces the slight ringing effect and limits noise enhancement. We also tested Wiener deconvolution in combination with the estimated RMFT, but the above expression turned out to be both simpler and on average better performing. The Wiener filter approach could possibly become more useful with a detailed analysis of the spectral properties of the image noise.

The complete procedure for RMTF estimation for each pair of n available optical setups utilizing images of m specimen and for generation of synthetic images of a goal quality comparable with that of setup j utilizing initial images acquired with a setup k is as follows:

Algorithm:

1. For each specimen S_i, $i = 1 \ldots m$, acquire one image I_{ij} for each optical setup j, $j = 1 \ldots n$.
2. For each image compute the modulus of its Fourier transform, $|F_{ij}| = |\mathcal{F}(I_{ij})|$. For each optical setup j, sum spectra for the m specimen images: $\sum_{i=1}^{m} |F_{ij}|$.
3. For each pair of n optical setups, form the ratio H_{kj} according to (4). Utilized values are the n sums computed in the previous step.
4. Generate images of a desired goal quality of setup j, starting from real images acquired with a setup k, according to equation (6).

4 Experiments

We evaluate the method on Papanicolaou (Pap) stained microscopy images of cervical cells. Biological material was supplied by the Regional Cancer Center (RCC) in Thiruvananthapuram, Kerala, India. Image acquisition of 13 Pap-smear specimen was performed using an Olympus BX51 bright-field microscope equipped with a Hamamatsu ORCA-05G 1.4 Mpx monochrome camera. The microscope light path was filtered using a 570 nm bandpass filter (20 nm pass-band). The microscope was fitted with an E-662 Piezo server controller and actuator (Physik Instrumente GmbH & Co. KG, Karlsruhe, Germany). This allowed Z-axis step control with a 0.1 μm resolution during image acquisition.

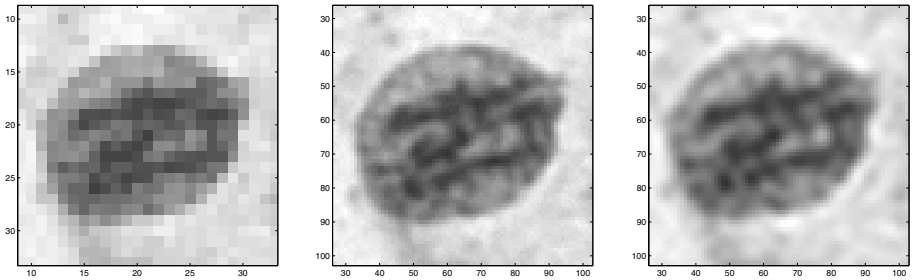

(a) 20x0.63 NA:0.75 (b) 40x1 NA:0.95 (c) Synthesized

Fig. 4. (a) Initial (sensed) low resolution image I_{ik}. (b) Reference image at desired goal quality I_{ij}. (c) Enhanced image $\tilde{I}_{ij}$ according to (6).

Each field of view was imaged at seven different resolutions, achieved through combinations between four objectives (20×, 0.40 NA; 20×, 0.50 NA; 20×, 0.75 NA; 40×, 0.95 NA) and two camera adapters (0.63×, 1.00×). The chosen combinations are listed in Table 1. Fields of view were imaged at 21 focus levels, spaced at a 0.2 μm offset, for each resolution. This assured that in-focus information is available over the entire image field. In total, 55 fields of view were acquired from the 13 specimen. A seeded watershed algorithm was applied to an extended depth of focus [2] image, generated from each focus stack, to segment manually marked nuclei, a part of such an image is shown in Fig. 1. Nuclei were then registered between resolution levels so that the same nucleus could be identified at all different resolutions. Fig. 2 shows one cell nucleus as it appears in the seven different microscopy configurations. The dataset is freely available and is documented in [8]. Cells close to the image borders were removed, leaving a total of 350 × 7 images. The data set is split in two halves, s.t. one part is used for

Table 1. List of objective and adapter combinations used to acquire images for the multi-resolution dataset and the resulting effective pixel size

Objective magnification	Objective NA	Camera adapter magnification	Effective pixel size (μm)
20	0.40	0.63	0.50
20	0.75	0.63	0.50
20	0.40	1.00	0.32
20	0.50	1.00	0.32
20	0.75	1.00	0.32
40	0.95	0.63	0.25
40	0.95	1.00	0.16

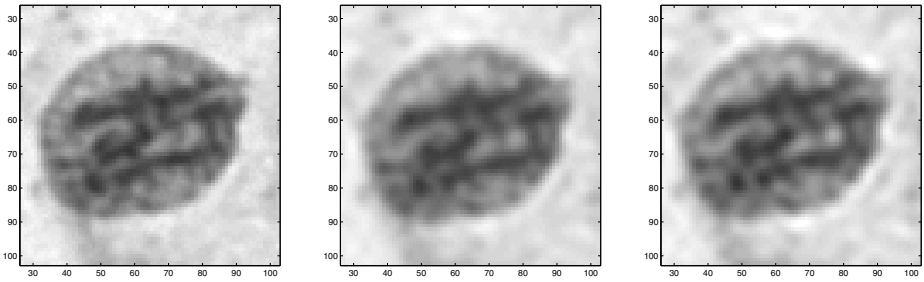

(a) Aligned reference, 40x1 NA:0.95

(b) Lanczos3 resampled from 20x0.63 NA:0.75. R=0.969, NMI=0.388

(c) Proposed method from 20x0.63 NA:0.75. R=0.993, NMI=0.550

Fig. 5. (a) Aligned reference image. (b) Lanczos resampled image. (c) Resampled image according to (6).

training (i.e. estimation of RMTFs) and the other part is used for performance evaluation.

RMTFs are computed as described in Section 3. We notice that for higher frequencies, which are essentially blocked by both of the involved optics, the RMTF approaches 1.0, seen as brighter corners in Fig. 3. As long as high frequent sensor noise is moderate, this does not lead to any problems; there is no large amplification of any frequency. Application of the Butterworth filter, as written in Eq (6), is therefore the only additional processing step we include.

5 Quantitaive Evaluation

Instead of relying on secondary estimated features, we perform a more direct evaluation by pixel-wise comparison of enhanced images with accurately registered images acquired at the goal resolution. For such an approach accurate registration is of utmost importance. We have used a combination of phase based registration followed by a simplex search to minimize weighted cross correlation in the spatial domain.

Our focus is on the highly textured chromatin pattern within the cell nuclei. That region is a small part of each image; to not bias the evaluation by the surrounding less textured cytoplasm background, we find important to use an appropriate weighting mask. For that purpose, we use the same 2D Hann window as when computing the RMFT functions (Sect. 2.1). By this weighting, we also reduce edge effects and further improve the precision of the registration.

The overall mean intensity and contrast values are not very informative for comparison of the type of images we work with. Since image intensities are not absolute quantitative for light microscopy images, standard pixel-wise distance measures such as mean squared error (MSE) and peak signal to noise ratio (PSNR) are not directly applicable. For image intensities normalized to zero

mean and unit variance, the MSE is equivalent to the Pearson correlation coefficient R, with a simple relation between them, $\text{MSE} = 2(1 - R)$. The correlation coefficient also corresponds to the structure component of the structural similarity index (SSIM), [13], (the other two components of SSIM are irrelevant for normalized images). These observations lead us to select the Pearson correlation coefficient as our first measure of similarity.

Another commonly used pixel-wise image similarity measure, which is insensitive to intensity and contrast changes, is normalized mutual information (NMI). NMI is a measure of the statistical dependence between two random variables. It can be qualitatively considered as a measure of how well one image explains the other. We use NMI as our second similarity measure, where the joint histogram of two images is computed using 64×64 bins, which gives a suitable quantization of the intensity scale.

5.1 Image Registration with Subpixel Precision

For useful pixel-wise comparison, the two images need to be perfectly registered. We apply a sub-pixel registration method proposed in [11] and further improved in [3]. This method operates in the Fourier domain and uses a refined DFT computation to estimate the peak in the cross correlation image with sub-pixel accuracy. The use of a log-polar transformation enables determination of rotation and scaling as well. Combined with a 2D Hann window, this method gives a fast and reasonably accurate image alignment. However, the used similarity measures are very sensitive to even the slightest misalignment and we observe that the log-polar phase correlation, due to near rotational symmetry of many of the nuclei, does not always provide high enough quality alignment for our purposes. We therefore perform a final sub-pixel refinement in the spatial domain, facilitated by a bounded Simplex optimization, which provides us the precision required.

5.2 Baseline Reference

To better appreciate the enhancement result, we evaluate how the two selected performance measures rank the similarity of repeated acquisition of the same cell, if the specimen is taken out of the microscope and put back, and then registered in the same way as our enhanced images. We consider a performed image enhancement successful if we reach a similarity with the target image which is not less that the lowest observed similarity by such repeated acquisitions of the same cell nucleus. Averaged results for 108 repeated acquisition are shown in Figures 6 and 7, for cross-correlation and NMI respectively, as semi-transparent surfaces intersecting the bar-plots. We expect that realistic variations due to imaging conditions are significantly larger than for repeated acquisition of the same microscope slide which does not involve variations in staining and operating conditions. We therefore find this selected baseline reference as sufficiently representative/demanding.

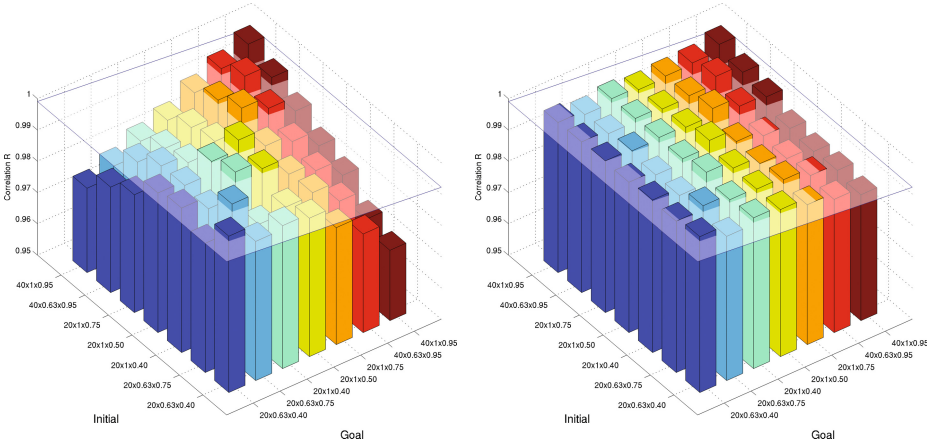

(a) Lanczos3 resampled (b) Proposed method

Fig. 6. Average correlation coefficients R between generated images and registered (ground truth) reference images, for all pairs of available initial and goal setups (qualities). (a) Lanczos resampled images. (b) Images generated according to (6). The semi-transparent plane corresponds the to lowest observed correlation between registered images of the same specimen, when repeatedly imaged without changing the optical setup.

5.3 Results

As an alternative to our proposed enhancement method, we observe resampling from one image resolution to the other using a Lanczos-3 interpolation. According to [1], the Lanczos kernel (with a = 3) keeps low frequencies and rejects high frequencies better than any other (achievable) filter seen so far. We find Lanczos interpolation comparable in terms of speed and complexity to the enhancement method we propose. We present and compare the computed weighted cross correlation and weighted NMI for both methods.

Results for the 175×7 images in our test set are presented in Fig 6 (correlation coefficients R) and in Fig 7 (NMI). Both measures lead to almost identical conclusion regarding achievable levels of image enhancement, by both observed methods Each bar in the presented bar-plots indicates similarity (correlation or NMI) between the enhanced initial image and the registered reference (goal) image for one particular combination of microscope setups. The enhancement method is successful (better than at least one repeated acquisition) if the transparent plane intersects the bar; in other words, all the bars with tops above the plain correspond to goal setups whose image quality can be reached by the corresponding enhanced initial setup. Clearly, the proposed method significantly outperforms Lanczos interpolation. The proposed fast and simple method provides a number of options for optimization in image acquisition and enables considerable reduction of image data (changing optics from 40×1 to 20×0.63

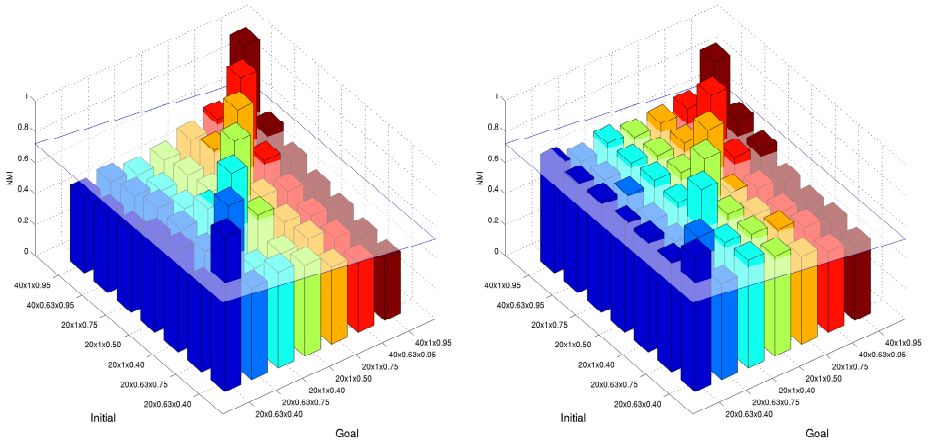

(a) Lanczos3 resampled (b) Proposed method

Fig. 7. Normalized mutual information (NMI) between generated and reference images, for all pairs of available initial and goal setups. (a) Lanczos resampled images. (b) Image generated according to (6). The plane corresponds to lowest observed correlation for repeated images of the same specimen.

results in more than a tenfold reduction of the image data), without sacrificing too much of relevant information.

6 Conclusions and Future Work

We have presented a method for microscopy image deconvolution, based on efficiently and accurately estimated relative modulation transfer function (RMTF). This simple and fast enhancement method enables generating images of higher quality, starting from those of lower quality, by a multiplication in the Fourier domain. We have evaluated the proposed method on a database containing cell images acquired by microscope setups of several levels of quality. We have performed pixel-wise comparison of the initial image, enhanced to the goal quality, with the registered image acquired by the setup having that goal quality, by observing correlation coefficients and normalized mutual information as measures of similarity. The tests show that the proposed method significantly outperforms the enhancement based on Lanczos interpolation and enables cost-effective image acquisition, since the desired quality of images can be achieved by the proposed subsequent processing at a high speed and low cost.

Acknowledgments. We are grateful to Dr K. Sujathan at the Regional Cancer Centre in Kerala, India for providing the cellular samples and to Dr Patrik Malm for making the used data set publicly available. J. Lindblad and N. Sladoje are supported by the Ministry of Science of the Republic of Serbia through Projects ON174008 and

III44006 of the Mathematical Institute of the Serbian Academy of Sciences and Arts. N. Sladoje is supported by the Swedish Governmental Agency for Innovation Systems (VINNOVA).

References

1. Blinn, J.: Jim Blinn's Corner: Dirty Pixels. Morgan Kaufmann Publishers Inc. (1998)
2. Forster, B., Van de Ville, D., Berent, J., Sage, D., Unser, M.: Extended depth-of-focus for multi-channel microscopy images: A complex wavelet approach. In: IEEE Int. Symp. Biomed. Imaging: Macro to Nano, vols. 1 and 2, pp. 660–663 (2004)
3. Guizar-Sicairos, M., Thurman, S.T., Fienup, J.R.: Efficient subpixel image registration algorithms. Optics Letters **33**(2), 156–158 (2008)
4. Joshi, N., Szeliski, R., Kriegman, D.: PSF estimation using sharp edge prediction. In: IEEE Conference on Computer Vision and Pattern Recognition, CVPR 2008, pp. 1–8. IEEE (2008)
5. Khare, A., Tiwary, U.S., Jeon, M.: Daubechies complex wavelet transform based multilevel shrinkage for deblurring of medical images in presence of noise. International Journal of Wavelets, Multiresolution and Information Processing **7**(05), 587–604 (2009)
6. Lindblad, J., Sladoje, N., Malm, P., Bengtsson, E., Moshavegh, R., Mehnert, A.: Optimizing optics and imaging for pattern recognition based screening tasks. In: Proc. Int. Conf. on Pattern Recogn., Stockholm, Sweden, pp. 3333–3338, August 2014
7. Malm, P.: Image Analysis in Support of Computer-Assisted Cervical Cancer Screening. Ph.D. thesis, Uppsala University, Department of Information Technology (2013)
8. Malm, P.: Multi-resolution cervical cell dataset. Tech. Rep. 37. Uppsala University, Division of Visual Information and Interaction (2013)
9. Oliveira, J.P., Bioucas-Dias, J.M., Figueiredo, M.A.: Adaptive total variation image deblurring: a majorization-minimization approach. Signal Processing **89**(9), 1683–1693 (2009)
10. Osher, S., Burger, M., Goldfarb, D., Xu, J., Yin, W.: An iterative regularization method for total variation-based image restoration. Multiscale Modeling & Simulation **4**(2), 460–489 (2005)
11. Reddy, B., Chatterji, B.N.: An FFT-based technique for translation, rotation, and scale-invariant image registration. IEEE Transactions on Image Processing **5**(8), 1266–1271 (1996)
12. Smith, E.H.B.: PSF estimation by gradient descent fit to the ESF. In: Electronic Imaging 2006, pp. 60590E–60590E. International Society for Optics and Photonics (2006)
13. Wang, Z., Bovik, A.C., Sheikh, H.R., Simoncelli, E.P.: Image quality assessment: From error visibility to structural similarity. IEEE Transactions on Image Processing **13**(4), 600–612 (2004)